

10.1

POST - A New Look at Stratocumulus

H. Gerber¹, G. Frick², S. P. Malinowski³, W. Kumula³, S. Krueger⁴

¹ Gerber Scientific, Inc, Reston, VA

² Naval Research Laboratory, Washington, D.C.

³ Institute of Geophysics, University of Warsaw, Warsaw, Poland

⁴ Dept. of Atmospheric Sciences, University of Utah, Salt Lake City, UT

1.INTRODUCTION

POST (Physics of Stratocumulus Top) is an aircraft field study conducted off the California Coast in July and August of 2008. A single aircraft,

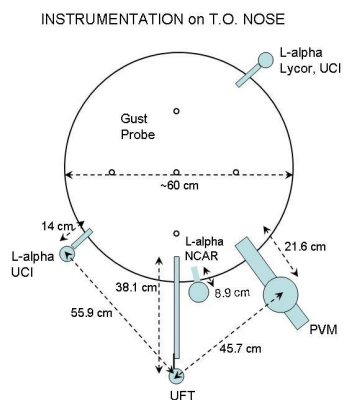


Figure 1 - Head-on view of the CIRPAS Twin Otter research aircraft showing the location of the UFT and PVM probes, and the Lyman-alpha probes which surround the 5-hole gust probe on the aircraft nose.

Corresponding author address: H. Gerber, Gerber Scientific, Inc, Reston, VA 20190; email hgerber6@comcast.net

the CIRPAS Twin Otter, was used to primarily investigate unbroken stratocumulus clouds (Sc) near cloud top. The aircraft was instrumented with a full suite of probes including probes for measuring state parameters of the atmosphere, drop spectra, CCN concentrations and spectra, radiation irradiances, and wind velocity and turbulence. A motivation to conduct another Sc field study in that region was the desire to apply lessons learned from the earlier DYCOMS II study of CA Sc of which the measured scale of entrained parcels were smaller than the critical probe separation, and the lengthy distance of the gust probe from these probes was too large. The Twin Otter (TO) aircraft permitted the close co-location of these probes to the gust probe on the aircraft; see Fig. 1. The Ultra-Fast Temperature (UFT) probe provided by the U. Of Warsaw (Kumula et al., 2010) and the PVM (liquid water content and effective radius; Gerber et al., 1994) provided high rate data to take advantage of the close separation ($\sim 1\text{m}$) to the gust probe. Both probes produced 1000-hz data, and their averaged 50-hz data is consistent with that separation at the TO aircraft speed of $\sim 50\text{ m/s}$.

The UFT and PVM as well as the whole suite of the other probes provided the first opportunity to look in detail at small scales that DYCOMS II taught us play a role in the Sc cloud-top physical processes. Unresolved questions include the role played by cooling at cloud-top caused by evaporation of cloud water due to the entrainment process. Is this cooling significant or negligible as proposed by Gerber et al. (2005)? What is the role of the Entrainment Interface Layer (EIL) in affecting entrainment? What affect does shear have near Sc top? How does the entrainment process affect microphysics? And, are such details required to understand the behavior and evolution of the Sc?

The TO flights originated from the CIRPAS facility at the Marina, CA airport located just north of Monterey. Seventeen flights were conducted off the coast in primarily unbroken Sc. The horizontal flight pattern of the TO is illustrated in Fig. 2. Ferry was

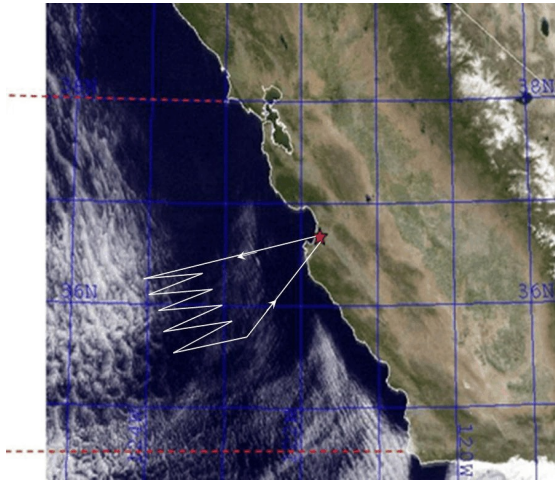


Figure 2 - NexSat image (courtesy Naval Research Laboratory, Monterey) of CA and the Pacific Ocean showing the typical horizontal flight track used for each quasi Lagrangian Twin Otter flight. The red star indicates the Marina airport near Monterey Bay.

followed by a quasi-Lagrangian zig-zag pattern that followed the mean air velocity in the Sc. All but two of the 17 flights used this pattern. A typical vertical flight pattern of the TO is shown in Fig. 3. The principal aspect of the vertical pattern were multiple “porpoises” through Sc top with the TO flying at a gentle angle up to about 100-m above and then 100-m below cloud top. More than 900 traverses of cloud top were made for the 17 flights. Additional parts of the vertical pattern included “flux runs” near the sea surface just below cloud base, and in the cloud. Also profiles much above cloud top were made.

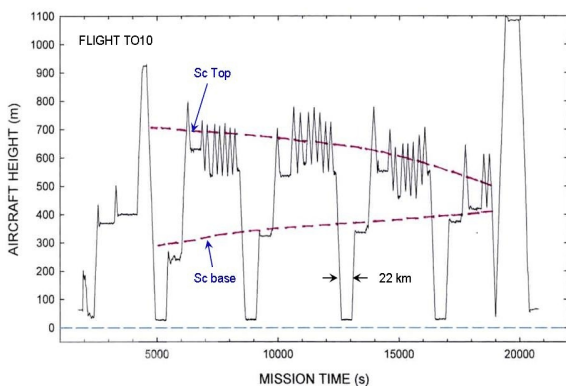


Figure 3 - Typical vertical flight pattern of the Twin Otter during POST flights. Porpoising through cloud top is the dominant feature.

About 2 dozen investigators from 1 dozen organizations participated in the field-phase of the collaborative POST effort. The reader is invited to visit the POST web site <http://www.eol.ucar.edu/projects/post/> for much greater detail than given in this brief introduction. This web site includes topics ranging from the submitted NSF POST proposal, to details of each of the TO flights, to the archived data that is freely available, and much more.

The following describes a limited aspect of the POST data analysis dealing with the entrainment process. Here we look at a small subset of the TO flights.

2. ENTRAINMENT PROCESS

It was noted in Gerber et al (2005) that parcels entrained into Sc top left an obvious signature of depleted LWC in the high-rate LWC record, and thus could be used to establish the geometry of these parcels, as well as estimate the mean entrainment velocity w_e into Sc top. Picking out these parcels (also called “cloud holes”) is termed “conditional sampling” where LWC is the “indicator variable”. The literature has numerous papers dealing with this approach. Other indicator variables such as DMS and ozone have been used.

Figure 4a shows the 50-hz LWC record for one porpoise through the Sc on flight TO10. Background values of LWC unaffected by entrainment are established by averaging the LWC record over 400-m, and 50-hz LWC values less than the average are considered the LWC in the entrained parcels (LWC in blue). Figure 4b shows the flux of depleted LWC’ (given by LWC in the entrained parcels minus the background average) multiplied by the deviation of the vertical velocity w' from the mean w . When both LWC’ and w' are negative (subsiding air) positive values result from the LWC’ x w' product which the data in Fig 4b mostly shows. The ellipse surrounds the data deviates from this trend. Here, surprisingly, LWC’ x w' is negative showing that this entrained parcel is rising.

Figure 4c shows the correlation between the 50-hz UFT temperature (T) and the depleted LWC’ parcels. The UFT data has been de-trended also using a 400-m average background temperature. The red part of the data indicates the T in the LWC holes shown in Fig. 4a. There exists a high correlation between values of cooled air (T') and the location of the LWC cloud holes.

Figure 5 shows an expanded portion of Fig.

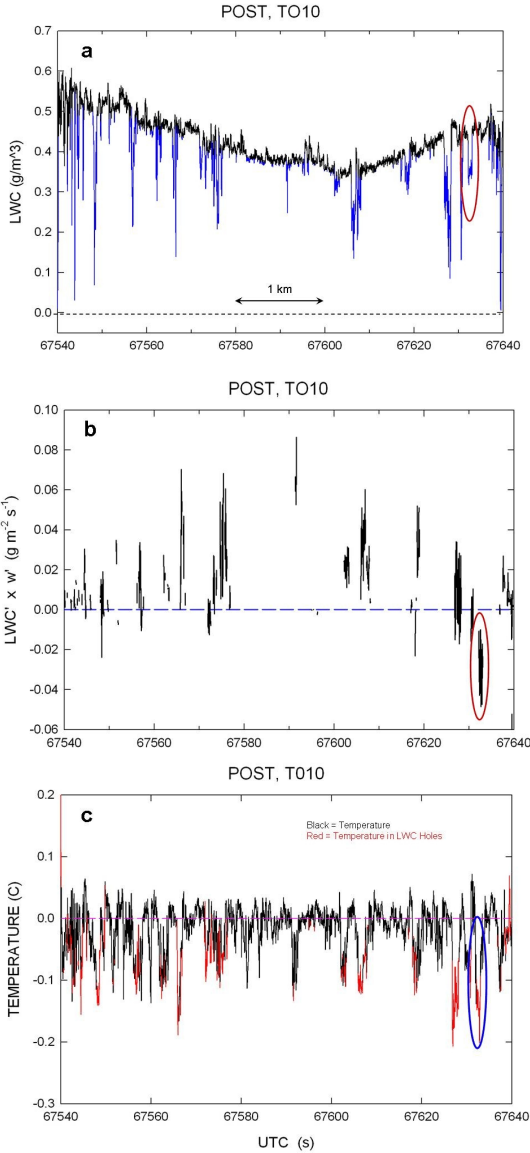


Fig. 4 - A 5-km segment of flight TO10 showing conditionally sampled “cloud holes in (a, blue lines), the flux of depleted LWC in (b), and the correlation between UFT temperature and cloud holes in (c).

4, with the numbers indicating the type of correlations found in the data. Most segments of T' show little or no LWC' (1), some show a partial contribution of LWC' (2), while others show the T' segment nearly full with LWC' (3). Two basic physical processes are at play to causing these effects: i.r. flux divergence cools cloud top, and cooling from LWC evaporated by entrainment can result in the negative temperature fluctuations. Given the greater frequency of the T' segments without substantial LWC' than those filled with LWC', it

appears that radiative cooling is the principal process; although, a significant contribution to cooling due to LWC evaporation can not be ruled out. Radiative cooling calculations at cloud top are needed to separate the two effects. It is interesting to note that another flight shows entirely different behavior: Malinowski et al (2010) finds positive T' in LWC holes near cloud top in flight TO13, which is attributed to strong turbulence/mixing.

The conditional sampling of LWC cloud holes as illustrated in Fig. 4 also permits the calculation of the pdf of the horizontal dimension of the holes vs the entrainment flux. Figure 6 shows this relationship for flight TO10 for all holes found between cloud top and 50-m below. The data illustrates approximate log-normal behavior which is also found in similar data for the other flights. However, the slope and geometric mean of the data differs for different flights, with the latter being substantially larger for some. This difference is not surprising, given the often different visual appearance of Sc top during the POST flights.

2. ENTRAINMENT VELOCITY

There are several ways to estimate the entrainment velocity, w_e . Here we give a sample of w_e calculations for a few POST flights using the conditional sampling method as described by Nicholls (1989). The following equation contains the parameters that need to be obtained from the data. A_r is the fractional area at cloud top covered by the entrainment holes (1), (2) and (3) are respectively the mean entrainment fluxes of depleted LWC' and the vapor mixing ratio q_v' , and q_T (4) is the total water mixing ratio jump above cloud top.

$$w_e = \frac{A_1}{A_1 + A_2} \frac{\langle w' \times q_T' \rangle}{\Delta q_T} = \frac{1}{A_r} \frac{\langle w' \times [(LWC' / \rho) + q_v'] \rangle}{\Delta q_T}$$

Figure 7 shows the depleted fluxes in the layer 100-m below Sc top for all of flights TO10 and TO6. In both cases nearly all of the depleted fluxes are positive, again indicating cooled entrained air descending in the cloud, in keeping with the classical concept (Nicholls, 1989) of conditional sampling of entrained parcels. However, near cloud top some negative values are found, as also suggested by Fig. 4. As expected the daylight flight has much smaller depleted flux values than the

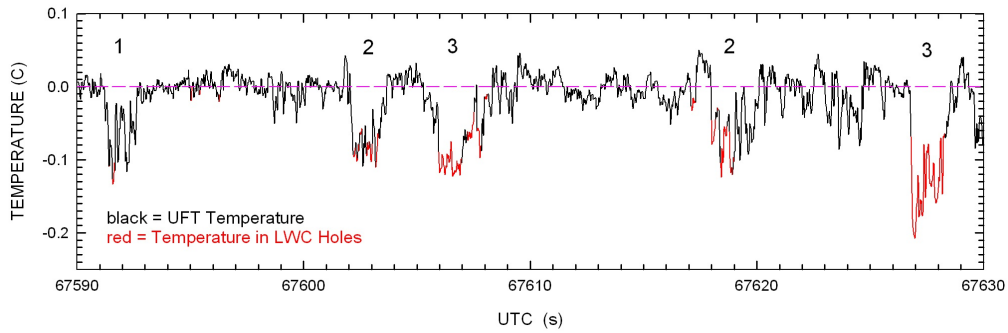


Figure 5 - A 40-s segment of Fig. 4 showing locations in the UFT temperature record that coincide with the depleted LWC in the cloud holes.

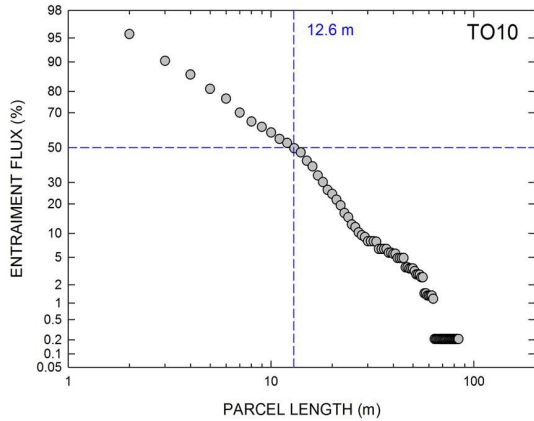


Figure 6 - Entrained parcel length vs entrainment flux for flight TO10.

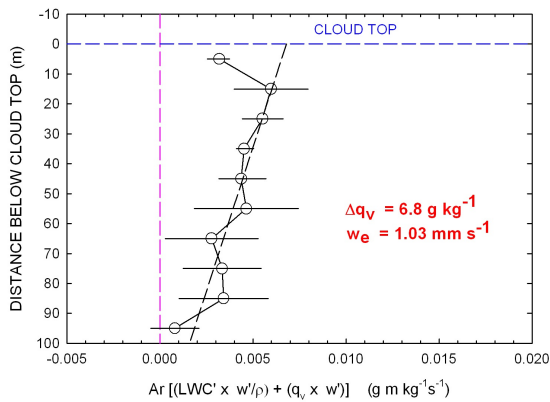


Figure 8 - Depleted flux times A_r averaged for each 10-m interval below cloud top for flight TO10.

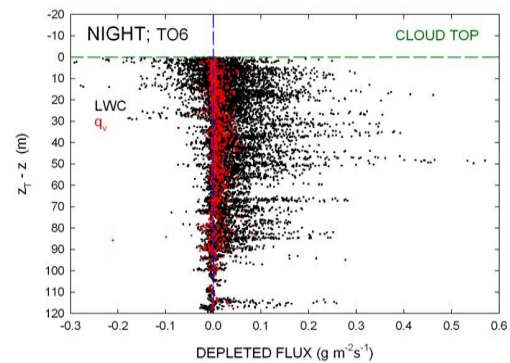
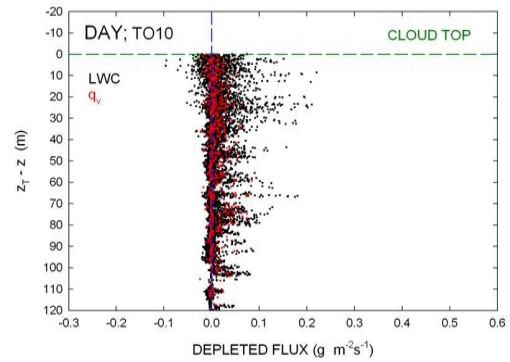


Figure 7 - The depleted flux in entrained parcels as a function of distance below Sc top for flights TO10 and TO6. The depletion of LWC (black) and q_v (red) are shown.

nighttime flight. In Fig. 8 the depleted flux data for TO10 is averaged over 10-m height intervals. The depleted flux decreases with distance below cloud top because the entrained parcels mix as they descend with the unaffected cloud. For this reason it is necessary to extrapolate the depleted flux values to cloud top. The vertical dependence of the fluxes is approximately linear for this flight, but is non-linear for some other flights. With the estimated q_v jump above cloud top of $\sim 6.8 \text{ g kg}^{-1}$, the above equation is used to calculate a mean value of $w_e \sim 1.03 \text{ mm s}^{-1}$ for flight TO10. The w_e calculations were done for each of the 15 quasi-Lagrangian flights with values of w_e ranging from $\sim 0.5 \text{ mm s}^{-1}$ to $\sim 8 \text{ mm s}^{-1}$.

Only about half the POST Sc flights showed classical entrainment behavior. Figure 9 for TO14 shows what can be termed non-classical behavior for the depleted entrainment flux. While the

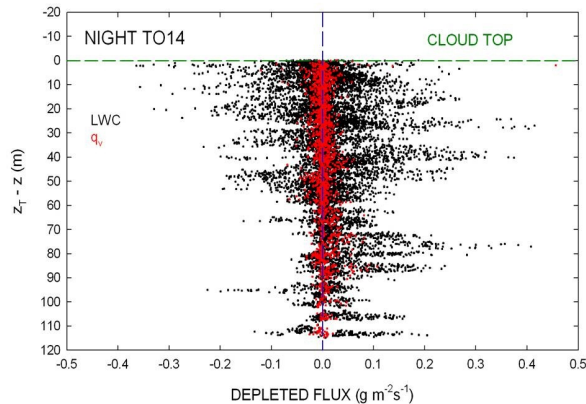


Figure 9 - Depleted flux for flight TO14 as a function of distance below cloud top. The presence of both negative and positive values indicates the presence of strong turbulence and mixing.

conditional sampling of LWC' still functions adequately for this flight, the data in Fig. 9 indicates nearly the same amount of LWC' ascending and descending in the top 60-m of this Sc. Using the data as shown in Fig. 9 to calculate w_e for TO14 results in nearly a zero value for w_e . If the LWC' in the entrained parcel is broken into smaller pieces by strong turbulence it will continue to exist until fully mixed with the rest of the cloud, whether it is moving

up or down in the cloud. Under this premise the negative flux values in Fig. 9 are assigned positive values and w_e is calculated to give $\sim 7.5 \text{ mm s}^{-1}$ for TO14. This procedure causes greater uncertainty in the w_e values. The following table divides the POST flights into classical, non-classical, day, and night categories.

Classical

Day	Night
TO9	TO6
TO10	TO12
TO16	
TO17	

Non-Classical

Day	Night
TO1	TO3
TO2	TO5
TO7	TO13
TO8	TO14
	TO15

The difference between classical and non-classical cases is clearly the degree of turbulence and mixing in the Sc. The likely cause for strong turbulence is wind shear near cloud top. The neglect of this effect in the conditional sampling approach to calculate w_e may have caused errors in the previously published values of w_e using this approach.

The higher resolution data provided by POST than previously available made it possible to calculate a set of entrainment velocity values (w_e) which in combination with the other measurements on the Twin Otter aircraft lead to hope that the parameterization of w_e can be improved from existing formulas. Such parameterization will also rely on ongoing analysis by POST colleagues described in Malinowski et al (2010), Hill et al (2010), Wang, Q., et al (2010), and Wang, S. et al (2010).

3. ACKNOWLEDGEMENTS

Appreciation is expressed to Hafliði Jonsson, Mike Hubbell, and the other personnel associated with CIRPAS for the exceptional support received during POST leading to a friendly and efficient atmosphere that produced an excellent data set. Stuart Beaton, Rob Wood, Tak Yamaguchi, and Arunas Kuciauskas are thanked for participating in the field study without POST funding, with Beaton fielding for the first time the new NCAR Lyman-alpha probe. Thanks are also due NCAR/RAF for working with POST P.I.s to establish the data archive. The support for the lead author was provided by NSF (ATM-0735121), NSF further supported other POST P.I.s, and the Office of Naval Research funded in part the cost of deploying the Twin Otter aircraft.

Wang, Q., M. Zhou, D.H. Lenschow, C. Dai, and S. Wang, 2010: Wind shear and thermodynamic characteristics near stratocumulus cloud top. *13th AMS Conf. On Cloud Phys.*, Portland, OR, 2010.

4. REFERENCES

Gerber, H., 1994: A new microphysics sensor for aircraft use. *Atmos. Res.*, **31**, 235-252.

Gerber, H., G. Frick, S.P. Malinowski, J.-L. Brenguier, and F. Burnet, 2005: Holes and entrainment in stratocumulus. *J. Atmos. Sci.*, **62**, 443-459.

Hill, S.A., S.K. Krueger, H. Gerber, and S.P. Malinowski, 2010: Entrainment interface layer of stratocumulus-topped boundary layers during POST. *13th AMS Conf. On Cloud Phys.*, Portland, OR, 2010.

Kumula, W., K.E. Haman, M.K. Kopec, and S.P. Malinowski, 2010: Ultrafast thermometer UFT-M: High resolution temperature measurements during Physics of Stratocumulus Top (POST). *13th AMS Conf. On Cloud Phys.*, Portland, OR, 2010.

Malinowski, S.P., K.E. Haman, W. Kumula, M.K. Kopec, H. Gerber, and S.K. Krueger, 2010: Small-scale variability of temperature and LWC at stratocumulus top. *13th AMS Conf. On Cloud Phys.*, Portland, OR, 2010.

Nicholls, S. 1989: The structure of radiatively driven convection in stratocumulus. *Quart.J. Roy. Meteor. Soc.*, **115**, 487-511.

Wang., S., Q. Wang, and A. Bucholtz, 2010: A large-eddy simulation study of observed stratocumulus clouds under weak inversion during POST. *13th AMS Conf. On Cloud Phys.*, Portland OR, 2010.